SUPPORTING INFORMATION

Elastic-instability enabled locomotion

Amit Nagarkar,[1,†] Won-Kyu Lee,[1,†] Daniel J. Preston,[1] Nan-Nan Deng,[1]

George M. Whitesides,[1,3,4,*] and L. Mahadevan[2,4,*]

[1] Department of Chemistry and Chemical Biology, Harvard University, 12 Oxford Street, Cambridge, MA 02138, USA.

[2] School of Engineering and Applied Sciences, Department of Organismic and Evolutionary Biology, and Department of Physics, Harvard University, 29 Oxford Street, Cambridge, MA 02138, USA.

[3] Wyss Institute for Biologically Inspired Engineering, Harvard University, 60 Oxford Street, Cambridge, MA 02138, USA.

[4] Kavli Institute for Bionano Science and Technology, Harvard University, 29 Oxford Street, Cambridge, MA 02138, USA.

[†]Authors contributed equally to this work

*Authors to whom correspondence should be addressed:

lmahadev@g.harvard.edu; gwhitesides@gmwgroup.harvard.edu

Methods

The buckling sheet actuator is based on a circular sheet of polycellulose acetate (an overhead transparency sheet) with a diameter of 20 cm unless otherwise noted. We attached a thin circular nylon film (Nylon film, 0.005mm, McMaster Carr) with a diameter of 5 cm to the centre of the sheet using double sided tape (3M 9589 double sided tape with polyethylene carrier material) to form a bladder. Thin tubing (PDMS, 0.5 mm internal diameter) connects the bladder to an external pneumatic source and the connection is sealed with a hot-melt adhesive (poly(amidoamine), Surebonder Glue Sticks) using a glue gun (Surebonder GM-160 Glue Gun, 10-watt). The transparency sheet and the bladder are both flexible but inextensible. When the bladder is pressurized, it expands in volume but contracts in diameter (due to its inextensible nature in the applied pressure range), applying tension to the entire transparency sheet. The cellulose acetate sheet releases tension by buckling out-of-plane. Upon the first actuation, the initial buckling instability created in the sheet occurs at a random position along the radial direction. The buckle can be directed by hand to the desired position. When this buckled sheet is kept in the buckled state for 10 minutes, the material develops a “buckling memory.” After this initial “programming” of the buckling position, the sheet always buckles reproducibly in the same location, making it a reliable actuator.

Fabrication of buckling-sheet actuator

Our actuator makes use of reversible bending of a material which is flexible but inextensible. We use cellulose acetate sheets (0.1 mm thickness, commonly used as substrates for presentations on overhead projectors). The modulus of elasticity of the cellulose acetate sheet was found to be 10 GPa (see Figure S2). This means that the sheet is practically inextensible at our working pressure (4 kPa over a circular area with radius 5 cm, with a strain of approximately 0.04%).

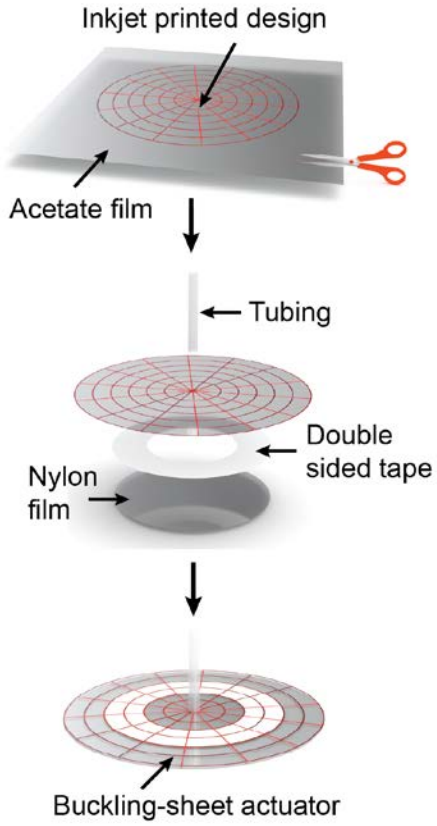

Figure S1: Fabrication process for buckling-sheet actuators. First, the circular design, i.e. the red stripes, of the buckling-sheet actuator was inkjet printed on a poly(cellulose acetate) sheet (an overhead transparency sheet), and the sheet was cut with a laser cutter. Then, a circular pneumatic bladder of nylon film was attached at the center of the designed acetate sheet with double-sided tape. Thin rubber tubing connects the bladder to an external pneumatic source.

Mechanical properties of the materials for buckling-sheet actuator

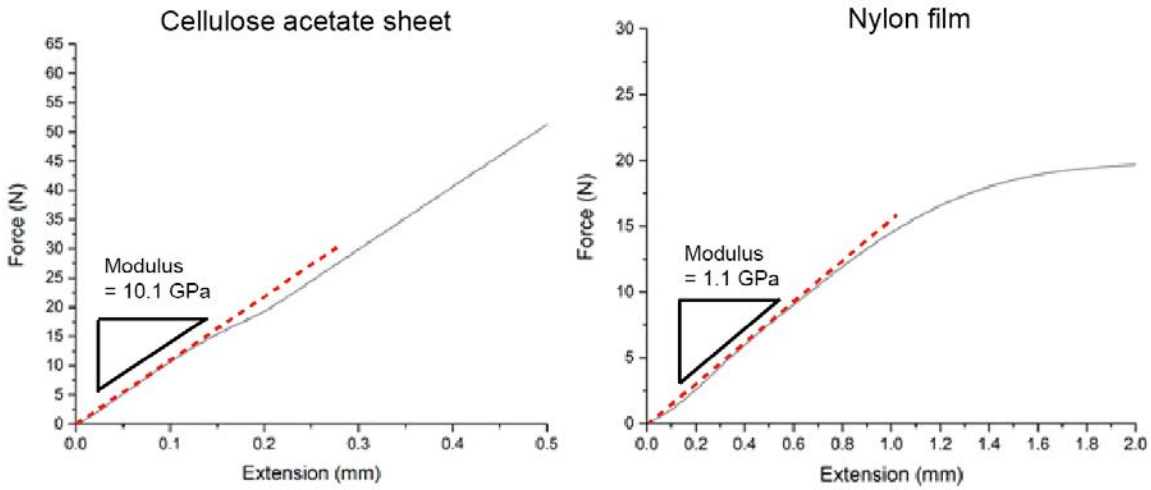

Figure S2. **Force-extension curves for the substrate material (cellulose acetate sheet) and pneumatic bladder (nylon film) for the buckling-sheet actuator.** The mechanical properties of the materials for buckling-sheet actuator were characterized by measuring force-extension curves for the acetate sheet (left) and the nylon film (right). The Young's modulus of the acetate sheet was 10.1 GPa and that of the nylon film was 1.1 GPa.

Experimental setup for the cyclic actuation of buckling-sheet actuator

The buckling sheet actuator was characterized with the experimental setup shown in **Figure S3** to generate the data provided in **Figure S4**. We varied the input pressure to the buckling sheet actuator with voltage-controlled pressure regulators (SMC Pneumatics ITV 0010-2BL for pressure above atmospheric, and ITV 0090-3BL for vacuum; reservoir gauge pressures indicated in **Figure S3**) interfaced to a computer with a DAQ (NI USB-6218 BNC), and we recorded the real-time pressure at the entrance to the buckling sheet actuator with an electronic pressure sensor (Panasonic ADP5151) connected to the same DAQ. The supply pressure was varied between 6.5 kPa above atmospheric pressure for 10 seconds and 20 kPa below atmospheric pressure for 10 seconds, for a total of 325 cycles in the present work, with minimal change in response of the bucking sheet actuator over the course of the experiment (**Figure S4**).

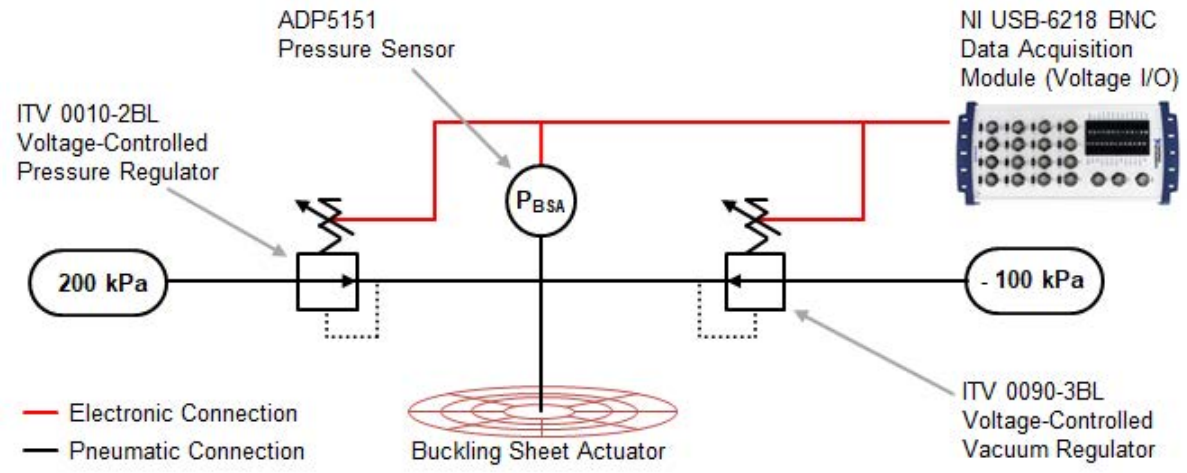

Figure S3: Experimental setup for the cyclic actuation of buckling-sheet actuator. Each soft pneumatic actuator was tested in the above experiment as shown. We varied input pressures with two voltage-controlled pressure regulators interfaced to a computer. We characterized and recorded input and output pressures with electronic pressure sensors connected to a DAQ.

Reliability of buckling-sheet actuator with cyclic actuation

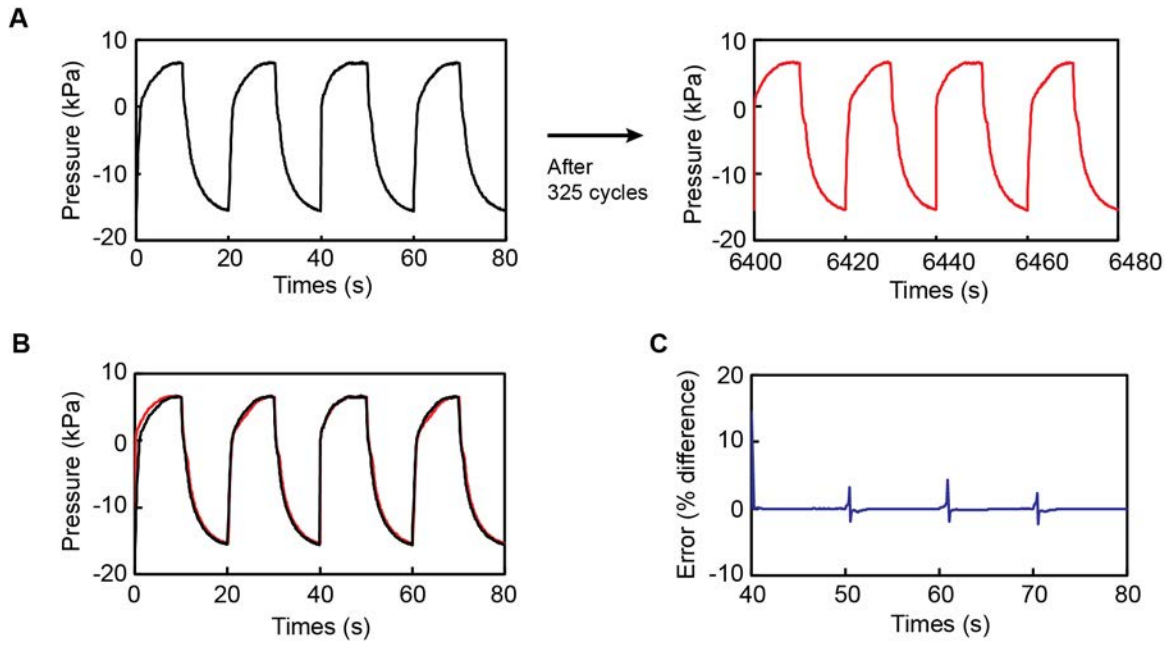

Figure S4. Cycling experiment results. (**A**) The actuator did not show any noticeable change in performance over the course of 325 cycles of pressurization and depressurization with 25 mL of air. **(B)** The buckling sheet actuator was pneumatically actuated 325 times with 25mL of air with no change in the pressurization curve after repeated actuation, which indicates that the actuation mechanism is robust and reproducible. Superimposed pressurization curves are shown before (black line) and after (red line) 325 cycles. **(C)** The difference between the initial pressure-time curve and the pressure-time curve after 325 actuation cycles.

Symmetry breaking by out-of-plane buckling

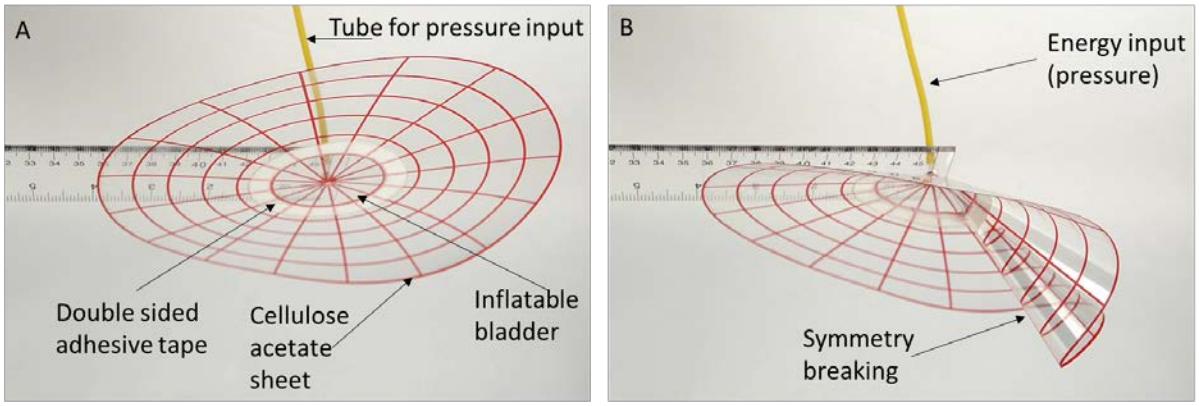

Figure S5. **Mechanism of symmetry breaking from the actuator.** (**A**) The buckling-sheet actuator consists of a flexible but inextensible cellulose acetate sheet and an inflatable bladder attached to the plane of the sheet. (**B**) Pressurization of the bladder induces stress and gives rise to out-of-plane buckles on the sheet. The initial buckling position is random, but once the buckle formed, the material creates a "memory" and subsequent buckling takes place at the same place.

Crawling motions of the buckling-sheet actuator with different design parameters

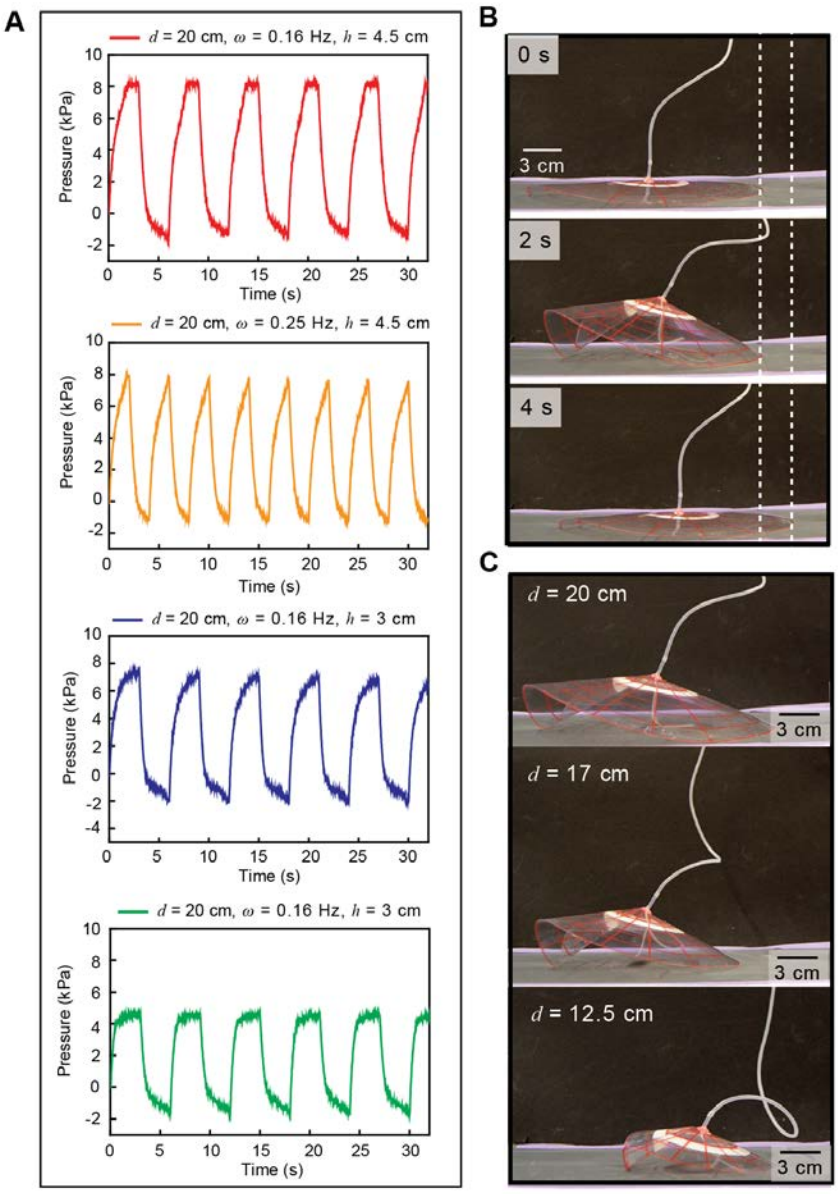

Figure S6. **Crawling motions with different *d, ω, h*. (A)** Graphs show the pressure as a function of time (with different combinations of *d*, *ω*, *h* values) during the crawling motion on the flat sandpaper. **(b)** Photos shows the locomotion from the single step of crawling. **(C)** Photos shows the crawling of buckling-sheet actuators with different *d* values.

Scaling law for the crawling motions of buckling-sheet actuators

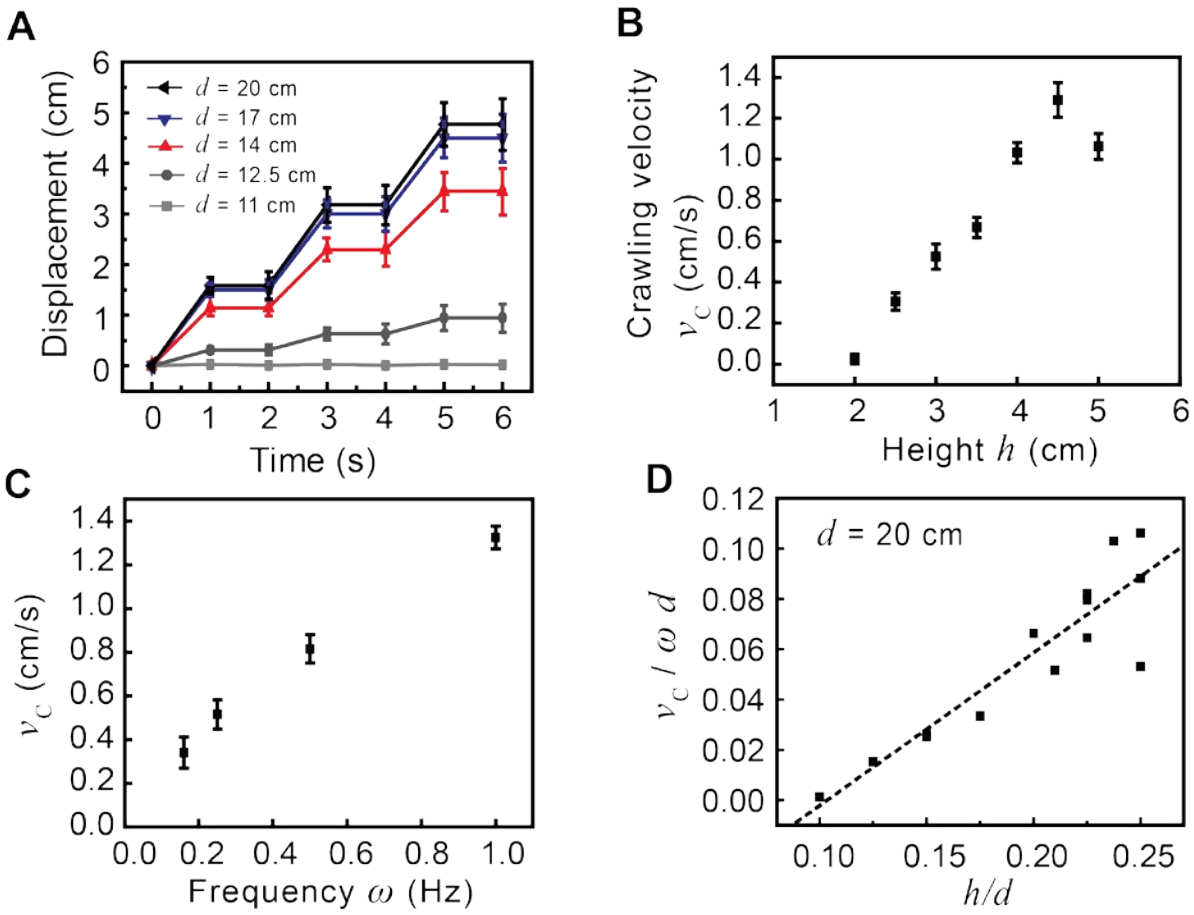

Figure S7. **Crawling motions of buckling-sheet actuator with scaling law in terrestrial environment. (A)** Displacement vs. time plot for crawling of the buckling-sheet actuator with different d values for ω = 0.5 Hz. **(B)** Plots of crawling velocity (v_c) as a function of maximum height (h) of the buckle when ω = 0.5 Hz and d = 20 cm. **(C)** Plots of v_c as a function of ω with d = 20 cm. **(D)** v_c / (ω d) vs. h plot to show the scaling law for crawling motions when d = 20 cm. All measurements were performed with pneumatic input for buckling of the sheet and vacuum for unbuckling of the sheet.

Scaling law for the swimming motions of buckling-sheet actuators

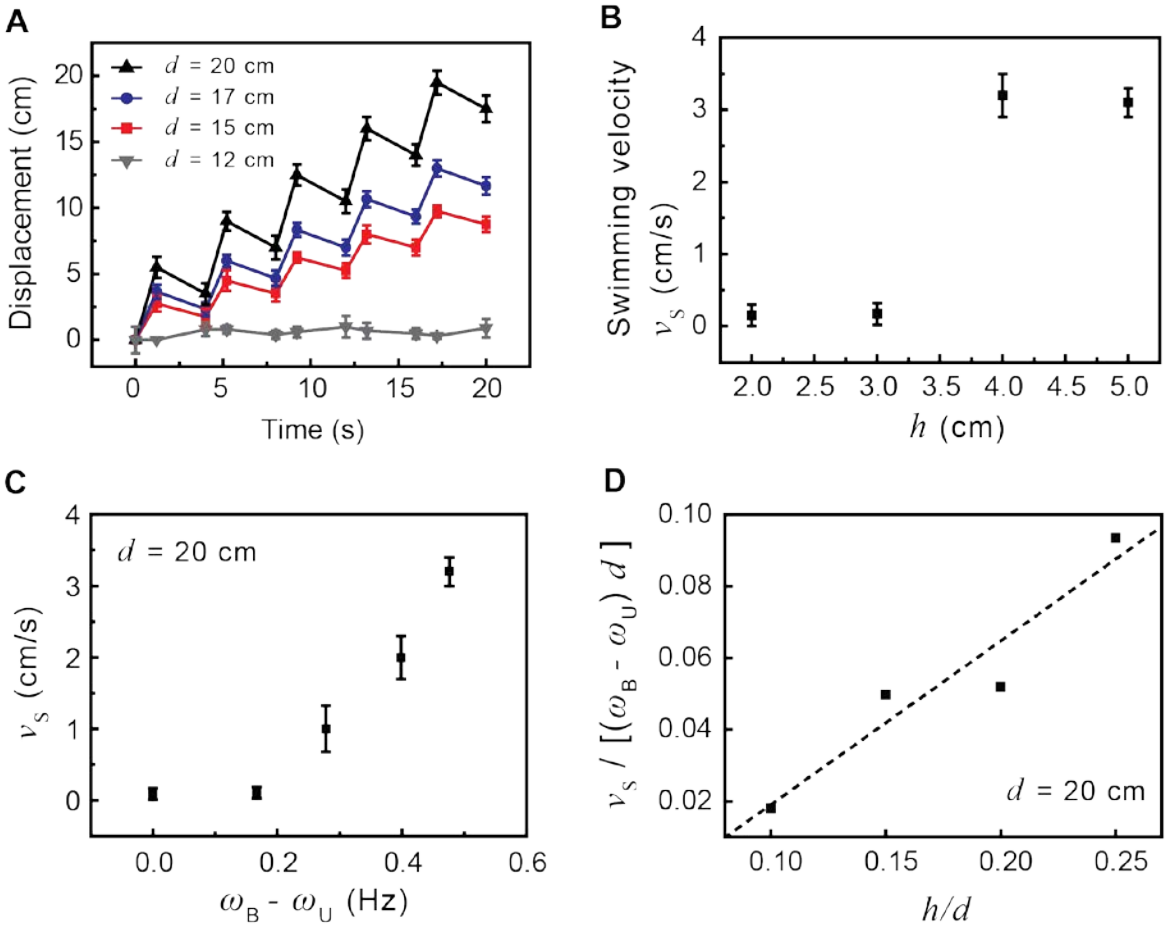

Figure S8. **Swimming motions of buckling-sheet actuator with scaling law in aquatic environment.** For swimming motion, the actuator with different diameters (d) was actuated with a constant buckling frequency (ω_B) and varying unfolding frequency (ω_U). **(A)** Displacement vs. time plot for swimming of the buckling-sheet actuator with different d values for $\omega_B \sim 0.83$ Hz and $\omega_R \sim 0.36$ Hz. **(B)** Plots of swimming velocity (v_c) as a function of maximum height (h) of the buckle when $\omega_B \sim 0.83$ Hz and $\omega_R \sim 0.36$ Hz, and $d = 20$ cm. **(C)** Plots of v_c as a function of ($\omega_B - \omega_U$) with $d = 20$ cm. **(D)** The plot of the scaling law for swimming, $v_S / [(\omega_B - \omega_U)\, d)]$ vs. h with $d = 20$ cm. For all measurements, the buckling frequency was $\omega_B \sim 0.83$ Hz.

Improvement in the efficiency of the locomotion system

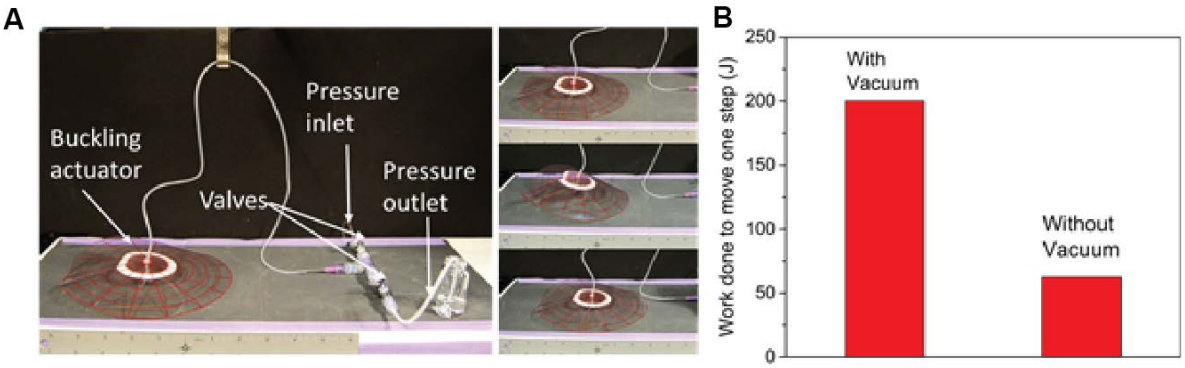

Figure S9. **Efficiency improvement with passive depressurization. (A)** The buckling sheet was actuated with a pressurization cycle and then allowed to equilibrate to air, removing the need for the depressurization cycle. **(B)** The plot represents the total work done to move the actuator through one pressurization–depressurization cycle.

Steering control

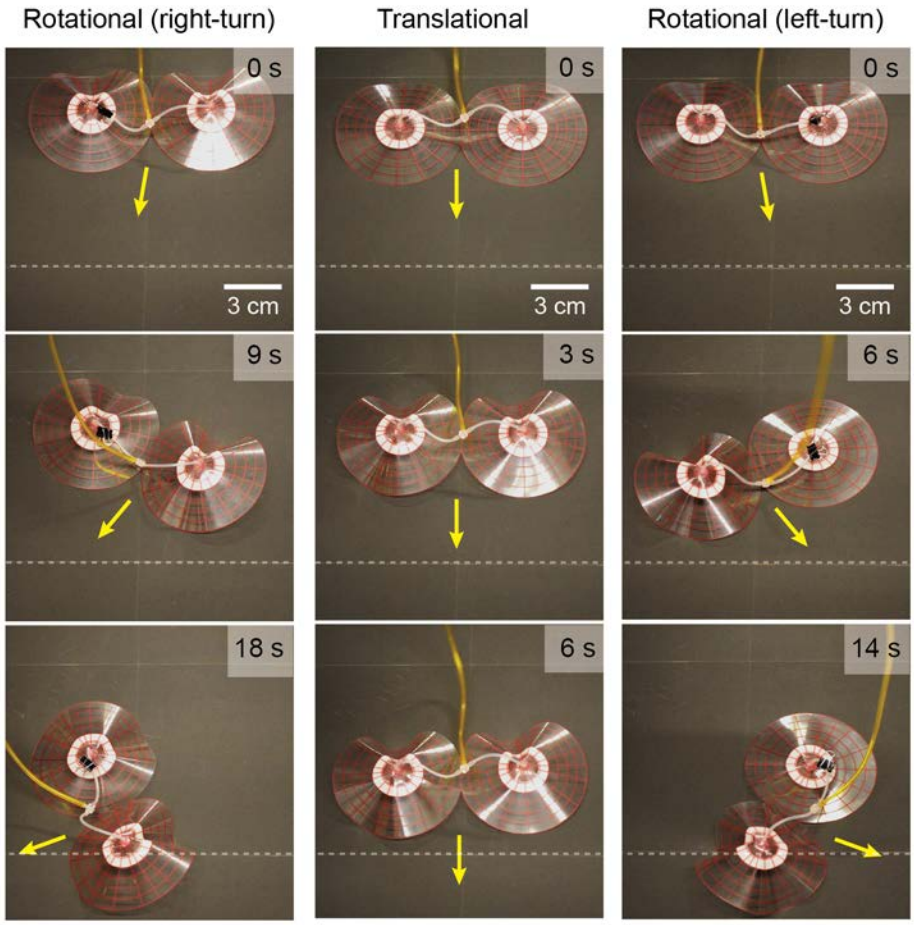

Figure S10. **Translational and steering motions from an actuator created using two buckling-sheet actuators.** Photos of translational and rotational motions from a single robotic system consisting of two buckling-sheet actuators connected in a symmetric configuration. The actuator was fabricated with a single cellulose acetate sheet with two pneumatic bladders to control two buckling instabilities independently. By actuating the two buckles simultaneously, the actuator travels in a straight line. By blocking one of the pneumatic tubes connected to the bladders, the robot turns left or right, giving rise to steering control.

Locomotion in confined environments

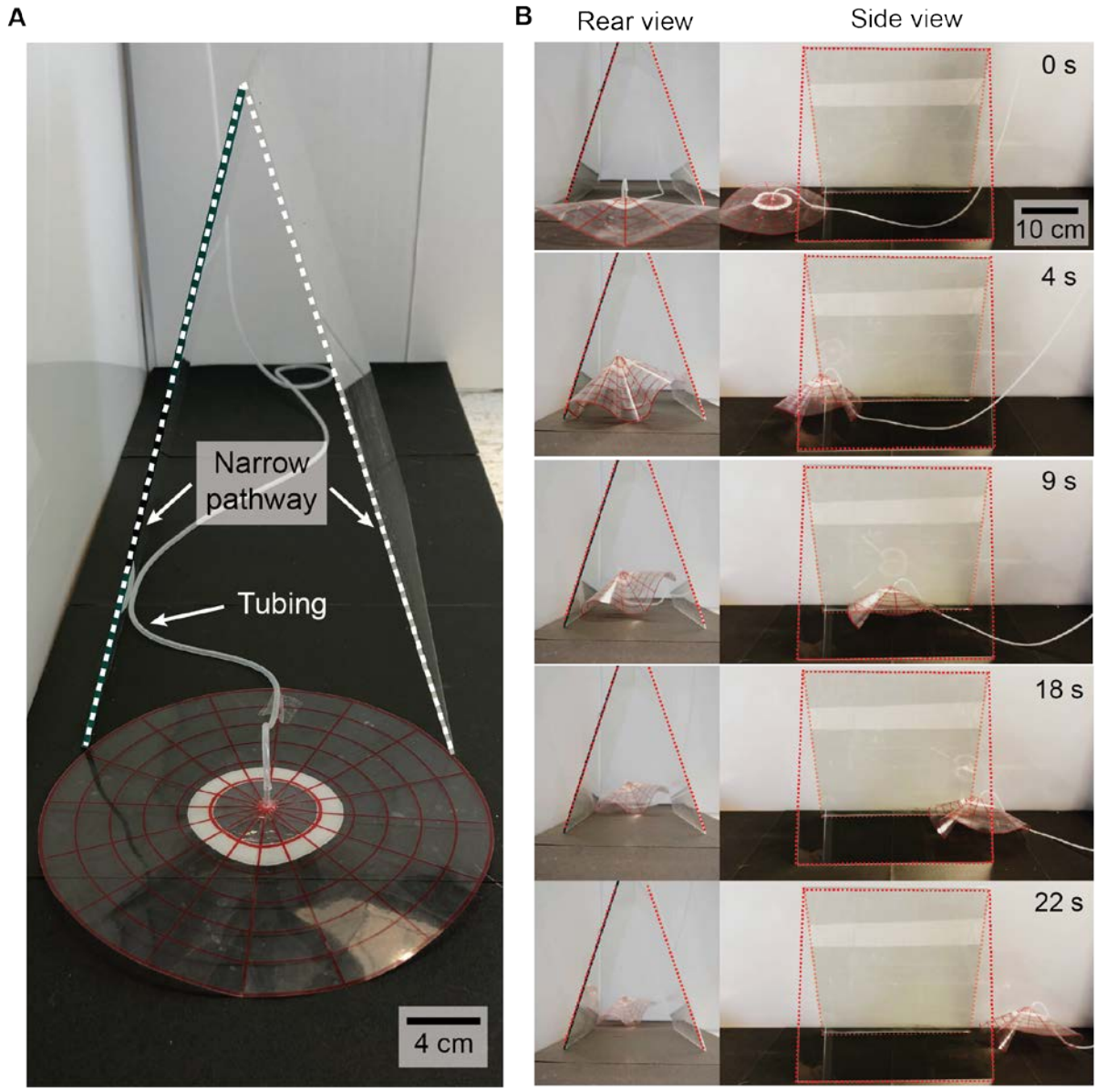

Figure S11. **Translational motion of buckling-sheet actuator in confined space. (A)** Photo of buckling-sheet actuator before entering a narrow pathway smaller than the diameter of the actuator (d = 20 cm, width of the pathway = 17 cm)**. (B)** Photos of the actuator squeezing through the narrow pathway and crossing the entire space (total length of 40 cm).

Captions for supporting information movies

Movie S1: Actuation of the conical-buckling animal ("Conimal")

Movie S2: Crawling of the conimal (d = 20 cm, ω = 0.5 Hz, h = 4 cm)

Movie S3: Crawling of the conimal (d = 20 cm, ω = 0.5 Hz, h = 2 cm)

Movie S4: Crawling of the conimal (d = 20 cm, ω = 0.25 Hz, h = 5 cm)

Movie S5: Swimming of the conimal when ω_B is larger than ω_U (d = 20 cm, h = 5 cm)

Movie S6: Swimming of the conimal when ω_B is similar to ω_U (d = 20 cm, h = 5 cm)

Movie S7: Translational motion of the twinned conimal

Movie S8: Steering motions of the twinned conimal

Movie S9: The conimal crawling through a confined space